

Article

Polystyrene Plastic Particles Result in Adverse Outcomes for *Hyaella azteca* When Exposed at Elevated Temperatures

Felix Biefel ^{1,2} , Susanne M. Brander ³ , Richard E. Connon ¹ and Juergen Geist ^{2,*} 

¹ Department of Anatomy, Physiology & Cell Biology, School of Veterinary Medicine, University of California Davis, Davis, CA 95616, USA; felix.biefel@tum.de (F.B.); reconnon@ucdavis.edu (R.E.C.)

² Aquatic Systems Biology Unit, TUM School of Life Sciences, Technical University of Munich, 85354 Freising, Germany

³ Department of Fisheries, Wildlife, and Conservation Sciences, Coastal Oregon Marine Experiment Station, Oregon State University, Newport, OR 97365, USA; susanne.brander@oregonstate.edu

* Correspondence: geist@tum.de

Abstract: Micro- and nano-plastics are pervasive pollutants in global ecosystems, yet their interactions with aquatic wildlife and abiotic factors are poorly understood. These particles are recognized to cause subtle detrimental effects, underscoring the necessity for sensitive endpoints in ecotoxicological exposure studies. We investigated the effects of particle uptake, size, and temperature on *Hyaella azteca*. Organisms were exposed to blue fluorescent polystyrene beads (500 nm and 1000 nm in diameter) at 0.43 mg/L for 96 h at temperatures mirroring climate predictions (21 °C, 24 °C, 27 °C). Besides survival and growth, particle uptake, visualized via confocal microscopy, and swimming behavior were analyzed. Mortality rates increased at 27 °C, and particle presence and temperature affected organism growth. Particle treatments influenced various behaviors (thigmotaxis, cruising, movement, acceleration, meander, zone alternation, and turn angle), with hypoactivity observed with 1000 nm particles and hypo- as well as hyper-activity responses with 500 nm particles. Particle uptake quantities were variable and increased with temperature in 500 nm treatments, but no migration beyond the gut was observed. Particle size correlated with uptake, and relationships with behavior were evident. Elevated temperatures exacerbated particle effects, highlighting the urgency of addressing plastic pollution in light of climate change for aquatic organism welfare and ecosystem health.

Keywords: locomotion; fluorescent microplastics; uptake; confocal microscopy



Citation: Biefel, F.; Brander, S.M.; Connon, R.E.; Geist, J. Polystyrene Plastic Particles Result in Adverse Outcomes for *Hyaella azteca* When Exposed at Elevated Temperatures. *Water* **2024**, *16*, 1360. <https://doi.org/10.3390/w16101360>

Academic Editor: Reynaldo Patiño

Received: 23 April 2024

Revised: 6 May 2024

Accepted: 8 May 2024

Published: 10 May 2024



Copyright: © 2024 by the authors. Licensee MDPI, Basel, Switzerland. This article is an open access article distributed under the terms and conditions of the Creative Commons Attribution (CC BY) license (<https://creativecommons.org/licenses/by/4.0/>).

1. Introduction

The first actual synthetic, mass-produced plastic called “Bakelite” was developed by Leo Baekeland in 1907 [1]. According to the OECD outlook for 2060, plastic leakage to the environment is projected to double to 44 million tonnes per year, while the build-up of plastics in aquatic environments will more than triple, exacerbating environmental and health impacts [2]. This waste can undergo further degradation into smaller particles (microplastics: MPs < 5 mm; nanoplastics: NPs < 1 µm; both categories: MNPs). Plastic particles of various sizes are considered a global pollution problem, though their environmental effects are often unknown. Primary MPs (e.g., those designed for commercial use) and secondary MPs (those resulting from degradation) are present ubiquitously across various environmental compartments, encompassing aquatic and terrestrial ecosystems and atmospheric and geographically isolated areas [3,4]. NPs represent a category of debris that remains relatively understudied and poorly characterized. However, paradoxically, they may pose the highest risk compared to other types of aquatic litter. This heightened risk stems not only from their capacity to penetrate biological barriers, but also from their extensive surface area, which could significantly influence the mechanisms of bioaccumulation and bioamplification of other pollutants [5]. Plants, for example, can function as

sinks for anthropogenic litter [6], and aggregation of plastic particles increases with rising temperatures and particle concentrations, deeming them either more or less accessible to certain taxa [7].

One of the earliest publications identifying plastic pollution as a “worldwide oceanic problem” was published in 1984 [8], depicting the detection of plastic materials during the 1970s in several aquatic, benthic, and planktonic samples, as well as describing impacts on seabirds and seals. Seasons and weather shifts influence litter accumulation [9], while plastic breakdown is driven by environmental conditions such as temperature, pH levels, ultraviolet ray exposure, and the effects of friction with rocks and sediment, wind action, and animal interactions; on being ingested by animals, enzymatic activity can result in further fragmentation into smaller particles [10–12]. Besides size, plastic particles can be categorized by shape, such as fiber, rod, ellipse, oval, sphere, quadrilateral, triangle, free-form, and unidentifiable [13]. In aquatic environments, the concentration, size, and shape of MNPs are the main properties influencing the uptake and consequential effects on organisms [14–16].

Synthetic MPs can exhibit pronounced adverse impacts relative to natural particles, with varying sensitivities observed across taxonomic groups [17]. Exceptions may occur, as evidenced by natural fiber types like hemp, which have been demonstrated to exert greater oxidative stress on mysid shrimp *Americamysis bahia* compared to synthetic fibers [18]. Among those effects, mortality is not a commonly observed effect of MP ingestion, presuming low risk at environmentally realistic concentrations [19]. However, sublethal effects have been described to include altered swimming behavior (*Daphnia magna*, [20]), development (*Xenopus laevis*, [21]), innate immune function (*Pimephales promelas*, [22]), liver inflammation (*Danio rerio*, [23]), effects on reproduction (*D. magna*, [24]), and growth (*Chironomus tepperi*, [25]). Thus, there can be indirect and potentially high risks at the population level. The factors mentioned above can further degrade MPs into NPs. NPs carry elevated ecological implications due to their augmented surface-area-to-volume ratio, leading to amplified vector effects for pollutants and bacteria, with smaller particles capable of passive membrane permeation and larger ones requiring active transport mechanisms [26,27]. MNPs can accumulate in the digestive tract, with particle size and shape influencing retention time and distribution within tissues [28,29]. Prior research indicates that larger particles, even those in the low-micron size range, can translocate the gastrointestinal tract, fillet, and livers of wild fish [30], bioconcentrate, and remain in tissues such as the gastrointestinal tracts, even after an extended period of depuration [31].

Fish and benthic macroinvertebrates exhibit complex ecological interactions within aquatic ecosystems, influencing nutrient cycling, trophic dynamics, and habitat structure [32]. Benthic macroinvertebrates are a group of organisms highly susceptible to the presence of MNPs in aquatic ecosystems. They are particularly vulnerable because they can readily ingest plastic particles in the sediment, an environmental compartment with high MP levels [33]. Amphipods and isopods are especially effective models for evaluating the potential toxicity of contaminants and pollutants because they serve as intermediaries between primary producers and higher-level consumers [34,35]. Consequently, their role as prey for fish introduces the potential for scale and magnification effects in the transfer of MP through the food web. *Hyalella azteca* (HA; Saussure, 1858) is widely distributed in aquatic ecosystems and can be easily cultured in laboratories [36,37]. They are epibenthic detritivores and a model test species recognized by the United States Environment Protection Agency (USEPA). HA are approximately 1 mm long and 0.04 mg in weight upon hatching, eventually attaining a maximum length of around 7 mm and 8 mg at maturity [38]. Given its ecological niche within the food web, HA is inherently predisposed to actively uptake and consume MNPs when present in its natural habitat. Studies using HA have demonstrated a gut retention of 24 to 28 h (tire wear particles, [39]).

Diverse plastics originating from industrial activities are introduced into natural ecosystems, notably aquatic environments. Polystyrene (PS), a thermoplastic polymer, was the first synthetic polymer shown to occur in coastal waters in 1970 [40], and is

now commonly found in aquatic environments, alongside polyethylene, polypropylene, and polyvinylchloride [41,42]. PS is a high molecular weight synthetic aromatic polymer derived from the monomer known as styrene, and commonly used for producing foam, cups, and containers [43]. Studies using HA have confirmed that PS fragmentation during ingestion and egestion is significant, while its ingestion also led to changes in enzymatic oxidative stress biomarkers [44,45].

Rising temperatures associated with global warming have significant implications for aquatic organisms and ecosystems. Temperature fluctuations can affect crustaceans' lipid, protein, and overall energy status [46,47]. Temperature and MNP effects can interact, thereby modulating their toxicity through diverse mechanisms. Studies have demonstrated that exposure to PS at varying temperatures can produce compounded adverse effects on *Artemia franciscana*, with higher temperatures resulting in reduced growth and increased mortalities [48]. Furthermore, an elevated temperature was shown to intensify the bio-concentration, immobilization, and oxidative stress effects of polyethylene MPs on *D. magna* [49].

In addition to traditional endpoints such as survival and growth, which are extensively utilized in ecotoxicological studies, recent publications have highlighted the use of photomotor assays measuring parameters involved in behavior (e.g., [50,51]). The behavioral assessment holds significant promise as a powerful tool in the field of aquatic toxicology and water quality monitoring [52,53]. Behavior, shaped by biotic and abiotic factors, enables organisms to respond to environmental changes, including contaminant exposure [54]. Stressors, whether acute or chronic, can adversely affect various behavioral aspects, such as feeding, which can ultimately influence survival and population dynamics [55,56]. Jacob et al. [57] reviewed differences in behavioral, sensory, and neuromuscular function indicators between control and fish exposed to virgin (not artificially aged or loaded) MNPs and revealed that the majority of endpoints demonstrated significant effects; boldness, exploration, activity, and locomotion were especially affected.

The objective of this study was to determine whether the experimental parameters of particle size (500 nm vs. 1000 nm) and water temperature (21 °C, 24 °C, 27 °C) influence survival, growth, and swimming behavior (video-based tracking), and to which extent MNPs uptake (fluorescence) might contribute to adverse effects. We primarily aimed to evaluate whether the quantity of PS uptake would affect locomotion, as PS exposure was previously shown to influence the feeding and swimming behavior of mysid shrimp *Neomysis japonica* [58]. The selection of the two bead sizes was based on their representation of both micro- and nano-categories, with limited existing literature on studies involving these particular sizes. Because temperature can change the uptake, elimination, and resulting effects on an organism, there is a need to study particle effects at different temperatures, especially in the context of global warming. We use HA, a species recognized for its sensitivity to environmental changes, and a model organism for assessing the risks associated with pollution, thereby indicating ecosystem health.

We hypothesized that (i): elevated temperatures influencing metabolic rates are predicted to increase particle uptake, leading to growth reduction and the manifestation of stress-related swimming behaviors; and (ii): due to the altered translocation ability of smaller particles, they are anticipated to demonstrate prolonged retention times, thereby exacerbating their detrimental effects.

Echoing proposals that knowledge derived from engineered nanoparticle toxicity research can inform risk assessments of PS particles [59], PS studies could prove invaluable in identifying knowledge gaps and research needs by providing a baseline for future toxicity investigations [60].

2. Materials and Methods

Animal husbandry and toxicity assessments were conducted following USEPA guidelines [61,62], with some adaptations.

2.1. Animal Source and Acclimation

Hyalella azteca were obtained from Aquatic BioSystems Inc. (Fort Collins, CO, USA) at age 4–5 days and placed, on arrival, in a 2 L beaker containing 1 L of the water they were shipped in, which was mixed with 1 L culture water (with 0.22 micron filtered well water diluted by 50% using MilliQ). They were then maintained at 24 °C in temperature-controlled chambers (Thermo Scientific Precision Model 818 and VWR, Thermo Fisher Scientific, Marietta, OH, USA) under a 16:8 h light/dark cycle. Following an initial 24 h habituation, individuals were separated into three 1 L beakers (120 individuals in each) for a further 24 h to increase the culture water content. Then, they were transferred to 500 mL of 100% culture water and brought to treatment temperatures (21, 24, and 27 °C) at a rate of 1 °C/day over a period of three days. Animals were maintained in water (culture water) so as to adjust water hardness to 180 mg/L CaCO₃. The resulting physicochemical parameters measured using a multi-meter (MultiLab 4010-3W, YSI Inc., Yellow Springs, OH, USA) were: pH 8.83, conductivity 946 µs/cm, dissolved oxygen 98.0% DO, salinity 0.4%, Total Dissolved Solids TDS 944 mg/L, Oxidation-Reduction Potential U –105.6 mV. Beakers were aerated using glass pipettes and covered with parafilm to avoid atmospheric contamination. Any dead organisms were removed daily. During acclimation, animals were fed daily with 3 mL/L YCT (Aquatic BioSystems Inc., Yeast, Cereal Leaves, Tetramin, produced in accordance with EPA recommendations [63], 1850 mg/L average total solids).

2.2. Particle Source, Particle–Food Preparation, and Concentration Determination

Polystyrene beads with a density of about 1.03 g/cm³ were purchased from Applied Microspheres GmbH (formerly BS-Partikel GmbH, Mainz, Germany) at a concentration of 5% m/m (see spectral absorption and emission graph of blue fluorescence in Figure S1). The surface composition of these unmodified PS beads consists of unaltered polystyrene without surface functionalization, potentially featuring negatively charged sulfonic acid end groups. These particle solutions were also used by Götz et al. [64,65]. Particle mean diameters were 519 nm (NPs) and 1294 nm (MPs) with blue fluorescence. Particle stock solutions consisted of 50 mL MilliQ water, 50 mL YCT food, and 100 µL of PS particles; gentle shaking for 10 min and vortexing were used to homogenize the solution before adding the calculated volume to each beaker of 100 mL culture water (Table S1) and either 500 nm or 1000 nm PS beads at a single concentration of 0.43 mg/L. In order to prioritize the assessment of uptake quantities, our experimental design excluded leachate devoid of particles. This decision was additionally informed by the lack of observed fluorescence translocation from the gut to surrounding tissue during our range-finding study.

At present, there is a lack of adequate quantitative analytical methods to evaluate NP concentrations in environmental settings. However, it is theorized that secondary NP concentrations are likely to escalate due to their release via fragmentation and degradation processes of larger particles in marine and freshwater environments. Based on mass conservation principles, estimates suggest that NP concentrations could reach levels 10¹⁴ times higher than those currently measured for MPs [66]. Relative to total plastic weight instead of PS particle counts, worst-case scenarios showed higher concentrations in the environment: in playa wetlands, USA, 5.51 mg/L [67]; Southwest Europe and East Asia, 0.32 mg/L to 1.89 mg/L [68–70]; and Taihu Lake, China, 30–50 mg/L [71,72]. Studies indicate that the transport and distribution of plastic particles are governed by solution chemistry, particle size, and mineral surfaces [73]. Consequently, variations in particle sizes potentially influence the formation of PS conglomerates, resulting in localized yet elevated PS concentrations. As suggested by Lee et al. [7], NP aggregation should increase, correlating with both particle concentration and temperature.

2.3. Exposure and Water Physicochemical Parameters

After acclimation, ten individuals were transferred into each 100 mL exposure beaker (3 beakers/treatment/temperature, N = 30 individuals/temperature/treatment). All surviving animals were used for growth measurements and uptake quantification. For locomotor

assays, a total of 9×24 -well plates were run sequentially on a single day to evaluate behavioral responses of 6 individuals/beaker, $N = 18$ individuals/temperature/treatment. During exposure, the three environmental chambers were used to regulate water temperature. The means \pm SEM for the exposure duration were 20.7 ± 0.1 °C, 23.9 ± 0.1 °C, and 27.1 ± 0.1 °C, respectively, measured using HOBO loggers (Onset, MA, USA) placed in additional beakers in each chamber (Figure S2).

Conductivity, dissolved oxygen, salinity, and pH were tested daily (Table S2); ammonia (RedSea, Houston, TX, USA) reached a maximum of 0.8 μ M, nitrite 0 ppm, and nitrate 40 ppm (API, Philadelphia, PA, USA) by the end of the exposure. Air samples did not show relevant MP contamination across the exposure time in the chambers. HA exposed to a single particle dose of 0.43 mg/L (500 nm: 64,000,000 p/mL; 1000 nm: 8,000,000 p/mL of the micro size 1000 nm) at the beginning of the 96 h exposure, i.e., there was no water renewal during the exposure, and continuous aeration contributed to oxygen supply and particle suspension homogeneity. The exposure concentration was determined with a prior range-finding study starting with the environmental relevance with the tested endpoints survival, growth, swimming behavior, and uptake at medium temperature (Table S1). Our objective was to identify a concentration capable of eliciting behavioral responses and observable particle uptake. Although the chosen concentration does not reflect ecological conditions directly, it allowed for a detailed examination of the mechanistic relationships among endpoints and revealed differences from controls compared to lower concentrations. Additionally, food particles were introduced in the primary investigation to enhance uptake further. Reported PS concentrations are nominal due to particle–food mixture interference with fluorometric and light microscopy evaluation.

During exposure, mortality, along with water physicochemical parameters, was recorded daily. At the conclusion of the exposure, specific groups of organisms were transferred using a transfer pipette into individual wells of a 24-well plate, ensuring careful handling, with three biological replicates (i.e., organisms were taken from three replicate beakers of each treatment) and six replicates (animals) from each beaker to (A) run behavior trials or (B) run behavior trials with subsequent individual confocal imaging for fluorescent particle uptake quantification via fluorescent pixel counting (three biological, three technical replicates). After the behavior trials, animals were euthanized on ice and stored in 3% paraformaldehyde for subsequent analysis.

2.4. Growth: Total Length, Capsule Length, and Dry Weight

Total length, defined as the length along the dorsal edge from the tip of the rostrum to the telson tip, and capsule length, defined as the distance from the tip of the rostrum to the posterior margin of the cephalon [74], were measured via image analysis using Fiji version ImageJ 1.53t [75,76]. Images were taken on a ruler using a Leica S8APO stereomicroscope (Leica Microsystems, Chicago, IL, USA) and Canon EOS Rebel T6 SLR camera (Canon, Tokyo, Japan).

For dry-weight measurements, empty and opened 1.5 mL microcentrifuge tubes were dried at 60 °C for a minimum of 2 h and were subsequently allowed to cool for at least 30 min within a desiccator at room temperature. After measuring the tube weights (Sartorius Quintix, Goettingen, Germany, with a readability of 0.01 mg), all organisms that were not utilized for individual confocal microscopy (later called Group (B)) were pooled from each respective beaker and relocated into the tubes to dry them for 24 h at 60 °C with the caps removed. After cooling down within the desiccator, the total weight was measured and divided by the number of individuals.

2.5. Locomotor Behavior Assay

Behavioral studies were conducted using a DanioVision Observation chamber (Wageningen, The Netherlands) and integrated steady flow of water set to treatment temperature via chiller (TECO-US, Terrell, TX, USA). A 35 min LD (Light:Dark) cycle test was performed with alternating light and dark cycles of 5 min, following protocols described

in Siddiqui et al. [77,78]. After the exposure, HA was pipetted into randomized wells of 24-well plates (Corning Costar, Corning, NY, USA, 24-well Clear, Product Number 3524). Organisms were habituated for 30 min in the climate-controlled exposure chambers of their treatment temperature before being transferred into the Noldus system for evaluation. The LD cycle protocol consisted of an acclimation time of 5 min, following three alternating light and dark cycles of 5 min durations. During behavioral trials, a recirculating water system was used to keep HA at the treatment temperature. It was observed that some individuals remained in the center close to the water surface without moving. These individuals were still analyzed, as no mortality was detected, and were active following mechanical stimulus. EthoVision XT 14 software (version 14, Noldus, Wageningen, The Netherlands) was used for video tracking. For correlation analysis, standard endpoints TDM (total distance moved) and thigmotaxis (“wall hugging”, avoidance indicator), which describes the ratio of staying in the outer (“hiding”) to inner (“boldness”) behavior as described before by Segarra et al. [51], and velocity were used. The further behavioral endpoints used were defined before [50,77,78].

2.6. Internalization

After 96 h of exposure, animals were euthanized on ice and stored in paraformaldehyde until whole bodies were transferred on a microscope slide with a cover slip. Fluorescent visualization was used to quantify the uptake of the PS beads. This approach is commonly used to make fluorescent particles visible and screen their location in a non-invasive way [79–85]. For this study, we used a Leica TCS SP8 STED 3X microscope (Wetzlar, Germany) and the LAS X software (Advanced Imaging Facility UC Davis, version 3.5.7.23225). Internalization of particles was measured using Image J 1.53t. However, particle uptake was evaluated through two different approaches.

2.6.1. Group (A): Imaging in 2D

To obtain preliminary insights into the overall PS uptake patterns and variability among individuals, specimens from each beaker were recorded. These recordings were conducted using the Leica microscope set to specific parameters (excitation wavelength: 405 nm, emission wavelength: 500 nm), capturing layered merged tiff images. This approach allowed for a comprehensive visualization of PS uptake across the sampled population (500 nm: 21 °C: N = 18, 24 °C: N = 11, 27 °C: N = 13; 1000 nm: 21 °C: N = 15, 24 °C: N = 10, 27 °C: N = 14). Using the ROI (region of interest) Manager, areas of interest were drawn around the gut region of each individual to measure positive pixels after setting up a color threshold (threshold color settings: Red 0 and 255, Green 0 and 255, Blue 0 and 254; method: Default, Threshold color: Black, Color space: RGB, with Dark background) and transforming the pictures to binary images.

2.6.2. Group (B): Imaging in 3D

A subset of samples, distinct from those utilized in the previous analysis (A), underwent in-depth analysis to deepen the understanding of uptake dynamics. We aimed to uncover potential associations between the quantity of particles internalized by a single organism and its respective locomotor activities. Therefore, high-resolution images recorded with the Leica microscope were used to assess the quantity of ingested particles in the gut region following locomotion assays. This allows us to assign effect results to one individual and analyze their correlation. With this subsample, which had already gone through the behavioral assays, three individuals from each beaker (N = 9) were investigated via confocal microscopy. An excitation wavelength of 405 nm and an emission wavelength of 500 nm were used to make blue, fluorescent PS beads visible, producing 8-layered z-stack images through their body. In ImageJ, pixels above a threshold were counted with the following settings/procedure: (1) image-zstack-maxprojection, (2) threshold-otsu-red and 81 to 255, (3) transformation to binary, otsu dark, tick black background and make new stack, (4) draw ROI around the gut region, (5) ctr + h to create a histogram, and (6) note 255 value from the

list. These images were also used to measure individuals' total and capsule length for the correlation analysis.

2.7. Statistics

To assess whether there were any significant differences across various treatments, we employed two-way ANOVA analyses along with subsequent Tukey multiple comparison tests. The normality of the endpoint data was examined using Shapiro–Wilk tests, while Levene's tests were utilized to assess the equality of variances. In cases where these assumptions were not met, particularly in instances involving mortality, behavior, and fluorescence data, non-parametric KW (Kruskal–Wallis tests) paired with Dunn's multiple comparison tests were employed. To evaluate survival outcomes comprehensively, we utilized Kaplan–Meier survival curves in conjunction with the Logrank (Mantel–Cox) test, which are widely recognized statistical tools for analyzing time-to-event data, particularly for survival times. The Kaplan–Meier method enables the estimation of survival probabilities over time while accounting for censored observations, providing a clear visualization of survival trends among experimental groups. Additionally, the Logrank test used assesses the equality of survival distributions between groups, allowing for the detection of significant differences in survival rates [86]. These statistical approaches were selected due to their robustness in handling survival data and their ability to yield meaningful comparisons and trend assessments within our experimental context. To investigate associations between nonparametric data endpoints, we employed a Spearman correlation analysis. Unless otherwise indicated, data are presented as mean \pm standard error (SEM); differences were called significant at $p < 0.05$; analyses and graphs were run with GraphPad Prism (Version 10.1.2, © 1992–2021 Graphpad Software, LLC) and Jamovi (Version 2.3.16.0).

3. Results

3.1. Survival and Growth

Survival of control organisms not exposed to particles at 96 h and at 21, 24, and 27 °C was above 95%. While temperature significantly influenced overall survival (KW, $\chi^2 = 6.68$, $p = 0.035$), it was not affected by particle treatment (KW, $\chi^2 = 5.06$, $p = 0.08$; Figure 1a,b). However, at 27 °C, both the 500 nm treatment ($p = 0.033$) and the 1000 nm treatment ($p = 0.043$) exhibited significantly lower survival rates than their respective controls, indicating some combination effect of temperature and particle. Additionally, at 500 nm, there was a significantly lower survival at 27 °C relative to 500 nm at 21 °C ($p = 0.033$). Similarly, the 1000 nm treatments at 24 °C showed significantly higher survival than at 27 °C ($p = 0.0430$). The combination of the highest temperature of 27 °C plus the exposure to PS particles was consequently shown to have adverse effects on survival. This adverse effect was supported by Kaplan–Meier survival curves, which were shown to be significantly different (Logrank Mantel–Cox test: $\chi^2 = 19.44$; $p = 0.0127$) with a significant trend (Logrank test $\chi^2 = 10.11$; $p = 0.0015$). Especially the survival curve of 500 nm treatments at 27 °C differed in comparison to controls ($\chi^2 = 5.008$; $p = 0.0252$).

Total length was significantly influenced by temperature (ANOVA, $F = 6.24$, $p = 0.003$) and particle treatment (ANOVA, $F = 6.93$, $p = 0.001$) (Figure 2a). Specifically, at 21 °C ($p = 0.008$), 24 °C ($p = 0.008$), and 27 °C ($p = 0.008$), the animals exposed to 1000 nm particles were shorter in total length compared to the respective controls. In contrast, 500 nm treatments were not different in total length compared to respective controls. In all treatments, however, animals were significantly ($p < 0.05$) longer at 24 °C compared to 21 °C. There were no differences in dry weight and capsule length (Figure 2b,c).

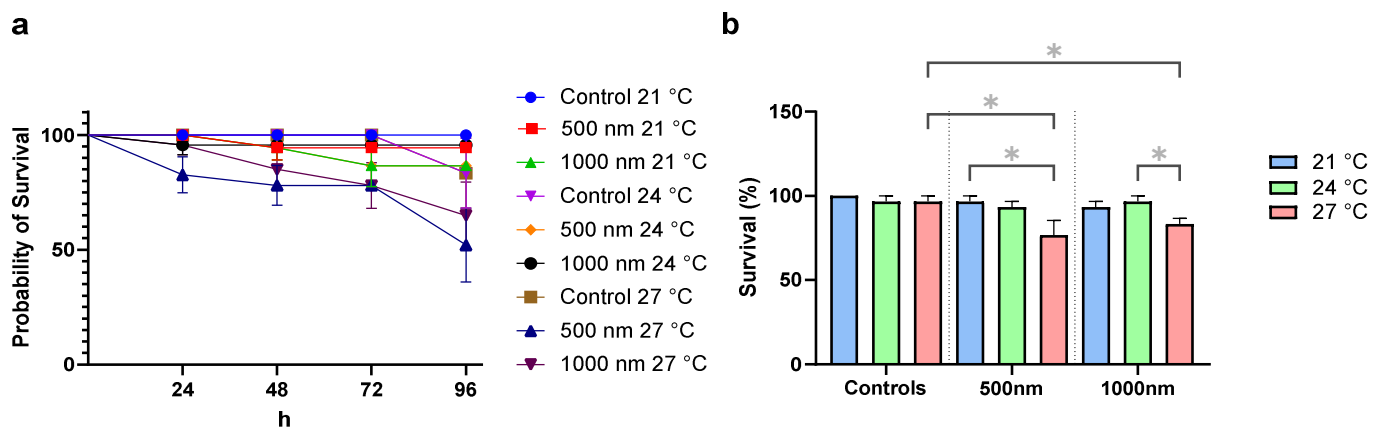


Figure 1. Survival during and after the 96 h exposure of *H. azteca* across treatments control, 500 nm PS particles, and 1000 nm PS particles at three temperatures (21 °C, 24 °C, and 27 °C). (a): Kaplan–Meier survival curve: probability of survival in percent (*y*-axis) over 96 h (*x*-axis). Survival curves are significantly different, with a significant trend. Survival curves differed at 27 °C between controls and 500 nm particle treatments ($\chi^2 = 5.008$; $p = 0.0252$). (b): Final survival rate at test termination in percent (*y*-axis) * $p < 0.05$, $N = 30$. (Mean \pm SEM).

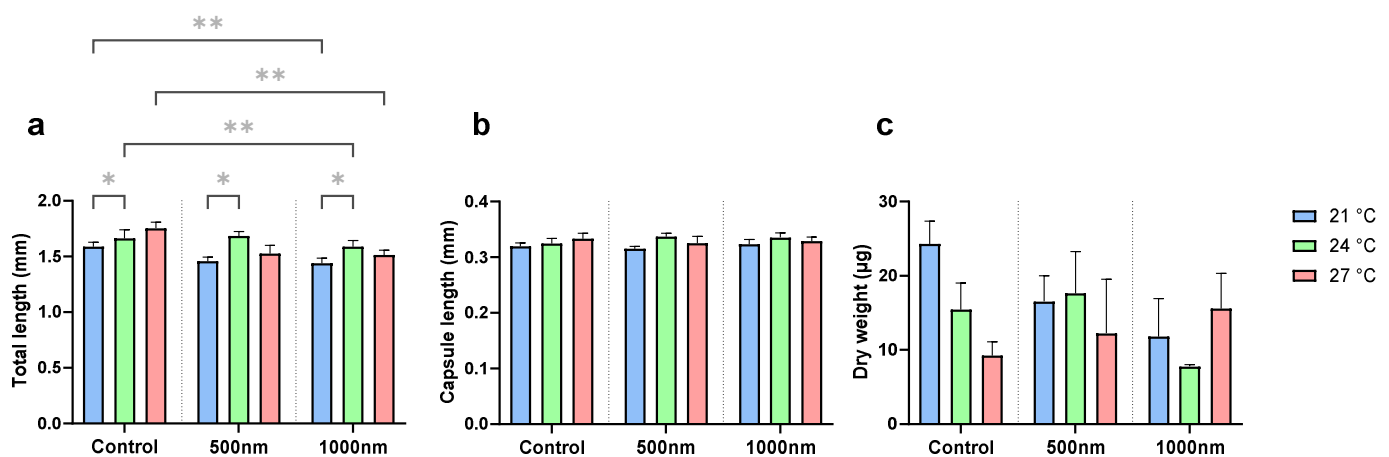


Figure 2. Growth of *H. azteca*: Total length (a), capsule length (b), and dry weight (c) (*y*-axis) ($N_{\text{dry weight}} = 2\text{--}3$) following 96 h treatments control, 500 nm PS particles, and 1000 nm PS particles (*x*-axis) and three temperatures 21 °C, 24 °C, and 27 °C. * $p < 0.05$, ** $p < 0.005$; $N_{\text{lengths}} = 11\text{--}21$. Total length was affected by particle treatment ($F = 6.93$, $p = 0.001$) and temperature ($F = 6.24$, $p = 0.003$). (Mean \pm SEM).

3.2. Locomotor Behavior Assay

The particle treatment significantly affected thigmotaxis, cruising, moving time, acceleration, meander, zone alternation, and turn angle ($p < 0.001$ for all endpoints; Table 1). Temperature influenced cruising ($p < 0.001$), moving ($p = 0.02$), acceleration ($p = 0.03$), and meander ($p = 0.04$) significantly. Interestingly, 1000 nm exposures led to hypoactivity, while 500 nm exposures led to decreased and increased behavioral activity endpoints. A Spearman correlation revealed that temperature was significantly correlated with TDM ($p = 0.03$ in dark, $p = 0.01$ in light) and velocity ($p = 0.03$ in dark, $p = 0.01$ in light) in controls, but not in treatments of animals exposed to particles (Table S3). Changes from dark to light cycles did not result in significant alterations to the behavioral parameters tested.

Table 1. Locomotor behavior assay of eight endpoints across PS particle treatment (control, 500 nm, 1000 nm), temperature (21 °C, 24 °C, 27 °C), and cycle (dark, light) after a 96 h exposure on *H. azteca*. A significant increase (↑) or decrease (↓) in comparison to the corresponding control treatment is marked in bold (Kruskal–Wallis, $p < 0.05$; N = 18). (Mean ± SEM).

Treatment	Temperature	Cycle		Thigmotaxis	TDM (mm)	Velocity (mm/s)	Cruising Mean	Moving Mean	Acceleration Mean (mm/s ²)	Meander Min (deg/mm)	Zone Alternation
Controls	21 °C	Dark	Mean	0.17	648.17	16,200.01	0.16	0.09	32.48	548,707.01	41.74
			SEM	0.04	77.73	1942.64	0.01	0.00	14.92	154,155.45	6.40
		Light	Mean	0.14	665.36	16,629.49	0.19	0.09	62.44	447,422.19	35.65
			SEM	0.03	80.66	2016.02	0.02	0.00	22.39	72,998.12	5.83
	24 °C	Dark	Mean	0.20	501.83	12,526.44	0.15	0.09	71.83	41,3407.62	56.02
			SEM	0.04	61.83	1543.29	0.01	0.00	18.13	67,852.27	7.44
		Light	Mean	0.20	528.67	13,196.59	0.15	0.08	26.67	568,502.63	58.46
			SEM	0.04	55.91	1395.66	0.01	0.00	9.78	130,905.13	7.16
	27 °C	Dark	Mean	0.33	447.96	11,172.90	0.17	0.10	56.47	510,822.34	77.50
			SEM	0.05	84.81	2115.36	0.01	0.01	20.02	269,753.60	10.82
		Light	Mean	0.28	495.26	12,352.93	0.19	0.09	75.39	775,993.28	74.13
			SEM	0.05	81.29	2027.59	0.01	0.01	30.74	263,831.07	10.38
500 nm	21 °C	Dark	Mean	↑ 0.32	↓ 394.47	↓ 9859.24	0.14	0.10	↑ 81.01	↓ 321,832.86	↑ 75.52
			SEM	0.05	44.41	1109.99	0.01	0.01	21.92	91,097.54	8.93
		Light	Mean	↑ 0.33	420.62	10,512.77	0.14	↑ 0.10	91.31	↓ 337,481.7	↓ 81.69
			SEM	0.05	54.43	1360.34	0.01	0.00	24.56	92,749.78	8.74
	24 °C	Dark	Mean	↑ 0.40	548.34	13,687.72	0.15	0.09	85.23	↓ 131,648.31	↑ 94.84
			SEM	0.05	88.12	2199.78	0.01	0.01	26.31	16,606.04	8.44
		Light	Mean	↑ 0.40	606.83	15,147.97	0.16	↓ 0.09	↑ 162.32	↓ 222,524.87	↑ 94.63
			SEM	0.05	101.73	2539.74	0.01	0.00	46.82	58,640.33	9.38
	27 °C	Dark	Mean	0.27	↑ 645.79	↑ 16,107.80	0.21	0.08	79.04	78,552,518.10	59.93
			SEM	0.04	84.73	2113.20	0.02	0.00	27.67	50,329,114.99	6.37
		Light	Mean	0.22	663.80	16,557.51	0.20	0.08	38.31	52,073,199.65	53.63
			SEM	0.04	85.59	2134.75	0.02	0.00	11.29	38,954,708.05	6.06
1000 nm	21 °C	Dark	Mean	0.26	↓ 460.38	↓ 11,506.56	0.15	0.09	90.86	288,840.77	56.74
			SEM	0.05	62.18	1554.11	0.01	0.01	27.82	46,682.69	8.55
		Light	Mean	0.27	↓ 475.73	↓ 11,890.01	0.14	0.09	77.79	↓ 307,032.33	61.56
			SEM	0.05	64.43	1610.24	0.01	0.01	24.39	48,446.12	8.92
	24 °C	Dark	Mean	0.21	642.22	16,030.16	0.13	↓ 0.08	55.44	368,102.43	47.63
			SEM	0.04	79.95	1995.47	0.01	0.00	14.53	68,938.96	7.91
		Light	Mean	0.21	697.79	17,417.42	0.14	0.08	53.18	↓ 316,204.54	51.54
			SEM	0.04	88.89	2218.80	0.01	0.00	14.26	65,979.64	7.84
	27 °C	Dark	Mean	0.28	487.30	12,156.83	↓ 0.14	↓ 0.08	54.77	566,070.12	58.57
			SEM	0.05	69.85	1742.71	0.01	0.00	17.89	257,837.42	7.38
		Light	Mean	0.28	508.36	12,682.07	↓ 0.13	0.09	57.39	332,440.14	61.65
			SEM	0.05	77.09	1923.03	0.01	0.01	18.50	67,763.56	8.43
Sign. category effect	Particle treatment			<0.001	0.82	0.82	<0.001	<0.001	<0.001	<0.001	<0.001
	Temperature			0.47	0.34	0.34	<0.001	0.02	0.03	0.04	0.28
	Cycle			0.49	0.47	0.47	0.81	0.60	0.48	0.59	0.96

3.3. Internalization

3.3.1. Group (A)

There was a notable variability in uptake across individuals within a single beaker. The guts of some individuals of the same replicate were filled entirely with PS beads, while others barely showed any fluorescence. Despite high uptake variability, treatments were shown to influence the measured fluorescence in the gut. Temperature ($\chi^2 = 7.47, p = 0.024$) and particle size ($\chi^2 = 17.7, p < 0.001$) had significant effects on uptake (Figure 3a), and

uptake at 21 °C was significantly higher in the 1000 nm particle treatments compared to 500 nm ($p = 0.0128$). Generally, it was observed that fluorescence in 500 nm treatments was lower compared to 1000 nm treatments, and that uptake variability was higher in 1000 nm treatments. The average range in 500 nm across all temperatures was 7.1%, and in 1000 nm treatments it was 26.3%. Linear regression revealed that the overall slopes of 500 nm and 1000 nm treatments, however, were not different ($F = 0.83$, $p = 0.46$), and the slope of 500 nm treatments was non-zero ($F = 162.8$; $p = 0.0498$), indicating increased uptake with temperature. Observationally, animals treated with 1000 nm particles also appeared to exhibit enhanced uptake with rising temperatures (Figure S3).

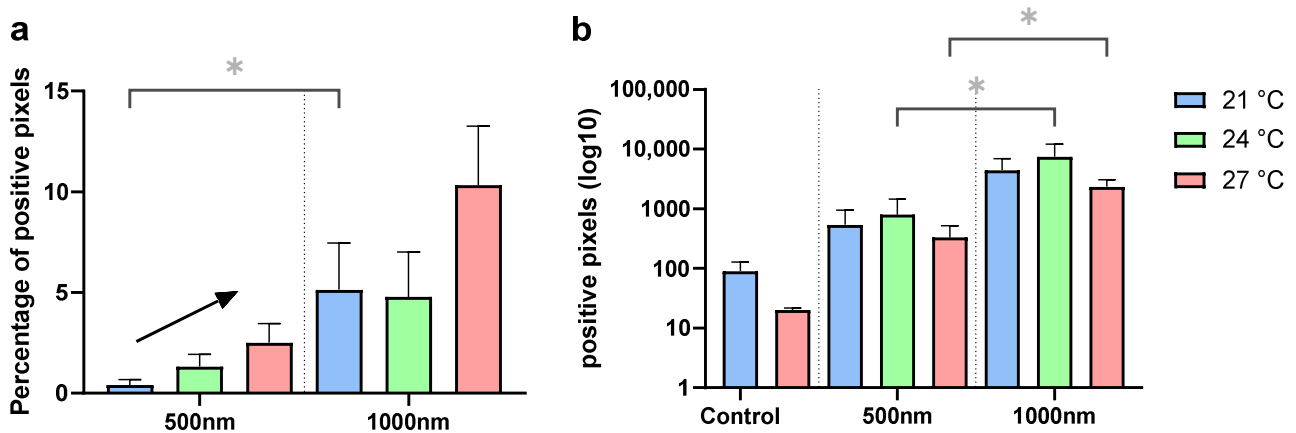


Figure 3. (a) Group (A): PS uptake comparison between the two investigated particle sizes of *H. azteca* by the percentage of positive pixels (y -axis) in relation to total pixel number in the ROI around the gut region. $n = 3$, $* p < 0.05$; 500 nm ($N = 11$ – 18), 1000 nm ($N = 10$ – 15). The increasing slope of 500 nm (arrow, $Y = 0.35 \times X - 6.99$) across temperature treatments is non-zero ($F = 162.8$; $p = 0.0498$). (b) Group (B): Logarithmic PS uptake of *H. azteca*: Pixels above threshold data (y -axis) across treatments control, 500 nm particles, and 1000 nm particles (x -axis) and three temperatures 21 °C, 24 °C, and 27 °C. $* p < 0.05$. Control ($N = 3$ – 6), 500 nm ($N = 8$ – 9), 1000 nm ($N = 9$). (Mean \pm SEM).

3.3.2. Group (B)

For animals that were maintained in clean water for 30 min acclimation and the duration of the behavioral assays, no significant differences in particle uptake quantity were observed in terms of temperature (KW, $\chi^2 = 2.38$, $p = 0.31$); in contrast, uptake quantity differed significantly between the particle sizes (KW, $\chi^2 = 34.56$, $p < 0.001$; Figure 3b). Consistent with the findings from (A), there were higher fluorescence signals in the 1000 nm particle treatments compared to 500 nm particle treatments. In total, 500 nm particle treatments at 24 °C ($p = 0.011$) and 27 °C ($p = 0.025$) exhibited significantly lower signals than the 1000 nm treatments at the same temperature. Examples of exposed animals are shown in Figure S4. Particle translocation from the gut was not observed in any surrounding tissues in any individual (Figure 4).

3.4. Correlations between Uptake, Particle Size, and Tested Endpoints

The strongest correlation was found for particle size and uptake (Figure S5). A Spearman correlation analysis was performed specifically for individuals which underwent the locomotion assay and the confocal analysis according to (B). Particle size and uptake demonstrated a r_s -value of 0.67 ($p < 0.01$). Furthermore, uptake correlated with TDM (dark) ($r_s = 0.35$; $p = 0.01$), thigmotaxis (dark) ($r_s = -0.28$; $p = 0.04$), velocity (dark) ($r_s = 0.35$; $p = 0.01$), TDM (light) ($r_s = 0.30$; $p = 0.03$), and velocity (light) ($r_s = 0.30$; $p = 0.03$). Total length was related to particle size ($r_s = 0.28$; $p = 0.049$) and temperature ($r_s = 0.02$; $p < 0.01$). The other endpoints were not correlated with the uptake quantity.

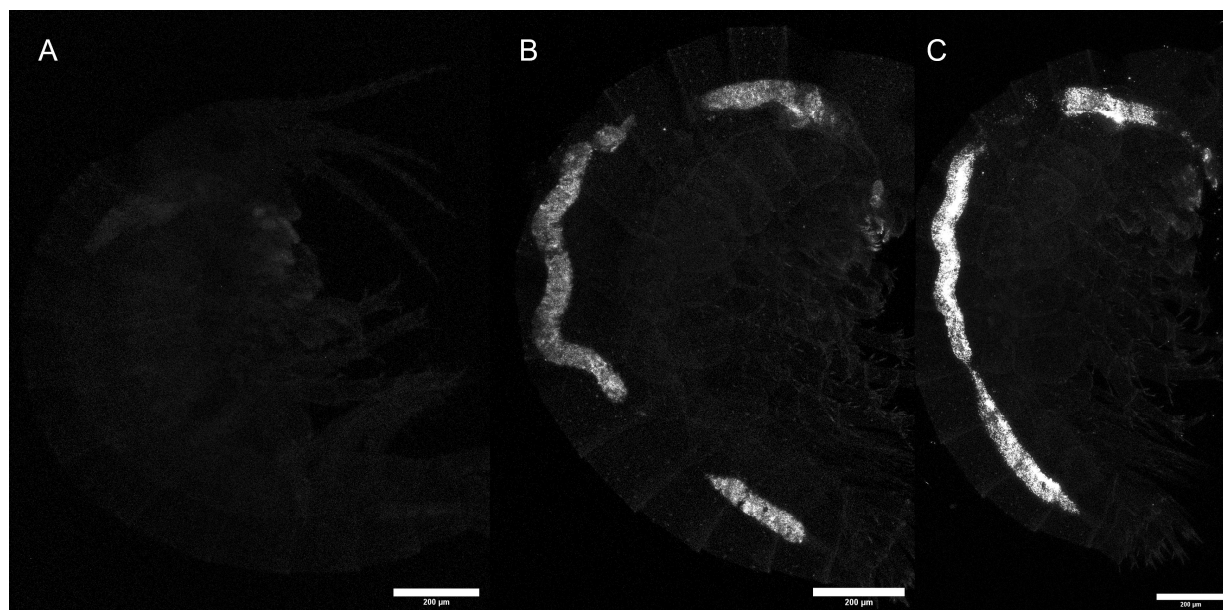


Figure 4. Internalization of fluorescent PS beads: control (A) and after exposing *H. azteca* to fluorescent PS beads with a diameter of 500 nm (B) and 1000 nm (C) for a duration of 96 h. Observations revealed a notable uptake in these beads distributed throughout the gastrointestinal tract of the organism.

4. Discussion

This study investigated impacts from exposure to micro- and nano-sized PS beads on uptake, locomotion, growth, and survival of the amphipod model species *H. azteca*. It also determined whether temperature would influence the measured effects. We hypothesized that elevated temperatures would lead to increased particle uptake, in turn leading to reduced growth and altered swimming behavior. This holds particular significance for smaller PS beads characterized by prolonged retention times, potentially attributed to factors such as increased probability of biodistribution and accumulation. Results confirmed our hypothesis (i) that elevated temperatures would increase particle uptake, resulting in decreased growth and survival. PS beads of 500 nm were not conclusively demonstrated to be more detrimental than 1000 nm beads in the context of survival and growth (hypothesis ii). The highest tested temperature of 27 °C, combined with 500 nm and 1000 nm PS beads at a concentration of 0.43 mg/L, led to harmful effects on HA. Besides survival curves exhibiting discernible temperature-dependent trends, total length exhibited significant alterations due to temperature and particle size. HA exposed to 1000 nm particles across all temperatures was shorter in total length compared to respective control groups. These results confirm findings in *A. franciscana*, which showed that besides higher PS concentrations, warmer water temperatures led to decreased survival and growth [48]. However, no differences in total length were determined between the 500 nm treatments and controls. The reasons might be that the larger-sized particles resulted in higher uptake due to a higher likelihood of confusion with food sources of similar size, such as yeast of 5 µm [87], which is part of the YCT food combination on which they were fed. It is interesting that although an apparent decline in dry weight was observed with increasing temperatures in the control group, this trend appeared to be absent in the exposure treatments involving 500 nm and 1000 nm PS beads. This discrepancy might indicate that the presence of these MNPs could potentially mitigate the effects of temperature on dry weight. Results also indicated that uptake increased with temperature and that behavioral effects differed depending on particle size.

Bead uptake could have reduced energy supply, leading to reduced total body length in 1000 nm treatments. Studies have demonstrated that *D. magna* reduces feeding rates when exposed to MPs [88]. The inhibition of metabolic rates due to exposure to MPs has been documented in various aquatic organisms [89,90], underscoring the capacity of

these minute pollutants to hinder physiological functioning. It also has been shown that microbiomes can be influenced by PS size in shrimp (*Litopenaeus vannamei*; [91]), which might further explain differences in growth and even in survival. However, it is worth mentioning that feeding rates have been reported to remain unaltered or even increase in freshwater amphipod *Gammarus fossarum* exposed to MPs [92] and that feeding rates can also vary over time [93]. Consequently, species' differences and adaptation mechanisms to food sources contribute to case-specific outcomes and can differ between our static exposure with no regular feeding and studies with regular feeding.

Both factors, temperature, and particle size, significantly influenced uptake quantities. Considering the correlation analysis of particle size, temperature, uptake, and total length, our results indicate that higher temperatures caused higher uptake and, ultimately, reduced growth and increased mortality. This result was confirmed by elevated temperatures demonstrating augmentation of the buildup of MPs within fish, consequently influencing the activity of metabolic enzymes [90]. Results are also supported by findings in the detritivores *Gammarus pulex* metabolic and feeding rates rising with larger body mass and higher temperatures, while MPs negatively impacted metabolic rates but not feeding rates [94]. As we observed high variability of particle quantities in the guts of HA, these differences between individuals of the same beaker could have led to high variability of growth and behavior responses. Per the manufacturer's specifications, an equivalent mass ratio of fluorescent dye to styrol was employed for both particle sizes. However, while the polymer weight was equal between 500 nm and 1000 nm treatments, the mean fluorescence intensity of PS beads was observed to scale approximately linear with the bead surface area, indicating that the brightness of spots declines as the bead size decreases [95]. Additionally, the ratio of volume to surface area might have influenced the signal, which could have further been affected by the number of particles (64,000,000 vs. 8,000,000 p/mL) and possible breakdowns in the organisms.

Elevated temperatures impose biological limitations on ectothermic organisms' metabolic and cellular processes [96,97] and increase metabolic rate, reaching the thermal optimum for a given organism, which can subsequently change individual feeding rates and induce modifications in interactions between consumers and resources [97–99]. Metabolic and feeding rates of *G. pulex* both demonstrated an increase in response to elevated temperature and body mass, in alignment with predictions from the Metabolic Theory of Ecology [96,98]. Based on the temperature coefficient or Q10 effect, biological reactions are influenced by temperature and, therefore, the energy status of organisms [46,47], leading to higher feeding demands at 27 °C, which could have caused higher uptake of particles. Increased mortality at 27 °C could have ultimately resulted from higher energy demand and PS beads, providing no nutritional value.

Studies suggest that HA has the capability to induce particle fragmentation attributed to its digestive system, characterized by a gastric mill for food crushing [45,100]. Higher metabolic rates and feeding demands at 27 °C might have caused particles to break down faster, which was not investigated in this study. However, this breakdown of PS beads could have led to a modification of effects over time due to particle dimension changes. For other organisms, smaller particle uptake has been shown to cause higher bioconcentrations and longer retention times [101], which could indicate higher stress-related effects of smaller PS particles. Similar to results on zebrafish showing that 250 and 700 nm particles barely passed the intestinal tract and outer epidermis [102], we did not observe apparent translocation into adjacent tissue leading to physical obstruction. Previous studies describe the necessity to add dye/leachate controls to the experimental design to determine if particles themselves, or the unrestricted movement of the dye molecule through cellular barriers, lead to fluorescence (e.g., [103,104]). However, we did not see fluorescence penetrating the gut wall, indicating that free leachate was absent.

Due to distinctive properties, such as hydrophobicity, plastics can adsorb contaminants (commonly called "vector" effect) of specific chemical properties, including persistent organic pollutants, amplifying the toxic effects on organisms [105]. Modified size-dependent

vector effects can explain growth and behavior differences between 500 nm and 1000 nm treatments. In this context, the volume-to-surface area ratio must be considered. Larger beads have a reduced surface area relative to their volume, and vice versa. As such, the larger surface of smaller particles would increase the likelihood of metabolites, bacteria, or other molecules conglomerating with 500 nm particles over 1000 nm. While the mass of PS was equal between the two size fractions, the particle count of 500 nm beads was also eight times higher than the 1000 nm beads. This would implicate an increased vector effect in 500 nm treatments, which could explain particle size dependent differences such as hyperactivity. Elevated temperatures may have facilitated bacterial growth, which could have further influenced vector effects. When PS was first detected in coastal waters, researchers found that the sampled particles had a high abundance of bacteria on their surface [40]. Growth rates of *Escherichia coli*, for example, exhibit a continuous increment from approximately 5 °C to its optimal temperature of around 37 °C [106], suggesting that bacterial growth or the metabolic byproducts thereof may have played a role in shaping the temperature-influenced outcomes.

Avoidance behavior might have been a reason for the high variability in particle uptake. For example, gastric filters of Atlantic ditch shrimp (*Palaemon varians*) can prevent significantly larger microparticles from reaching the midgut gland because they can filter and finally egest them [107]. The extent to which HA can accomplish this remains unclear. Still, some filter mechanisms and avoidance behavior are likely, which could explain individuals with little particle uptake supported by considerable variability in individual feeding rates, which has been described before [108]. Measured uptake quantities after locomotion assays did not increase with temperature. Locomotion assays, which took place in clear water, could have contributed to egestion, which can happen within two hours [79]. The process of removing animals from the exposure beaker, acclimation time, behavior trials, and euthanization spanned approximately 90 min, during which handling and light stimuli potentially heightened levels of activity and clearance.

In the context of behavioral characteristics, particle treatments, and temperature have demonstrated significant effects on various behavioral endpoints. Of the eight investigated behavioral endpoints, six were significantly influenced by particle treatment, four by temperature, and none by light:dark cycle change. Interestingly, exposure to 1000 nm particles elicited only hypoactivity-related locomotion, while exposure to 500 nm particles yielded an intricate interplay of hypo- and hyper-activity. The 500 nm treatments additionally led to 10 more significant behavioral effect differences to corresponding controls than 1000 nm treatments. This result can lead to the conclusion that the mode of toxic action is particle size dependent. Behavioral differences might furthermore be connected to non-significant but lower average survival rates of 500 nm treatments ($76.7 \pm 8.8\%$) compared to 1000 nm ($83.3 \pm 3.3\%$) treatments at 27 °C (across all temperatures $89 \pm 4.2\%$ and $91 \pm 2.6\%$, respectively). In the treatment with the highest mortality (500 nm, 27 °C), TDM and velocity were significantly higher than in the corresponding controls, indicating hyperactivity. Hyperactivity represents an escape response, functioning as a form of avoidance that serves as an adaptive reaction to evade stressful circumstances [109]. In contrast, in 1000 nm treatments at 27 °C, cruising (fraction spent at a speed of >0.5 mm/s and <20 mm/s) and moving time (fraction spent actively swimming) were reduced in darkness, indicating hypoactivity. This result, combined with reduced total length in 1000 nm treatments, corresponds with a reduction in body length (and oxidative stress), standing out as the primary factor contributing to hypoactivity in zebrafish [110]. Links between growth and reduced swimming activity in response to 15 μ m PS beads have also been described for jacobever (*Sebastes schlegelii*, [111]). The reasons for particle-size and temperature-dependent locomotion differences can be various. According to several studies [112,113], physical stress is the primary factor contributing to MP toxicity if the plastics do not contain additives or adhere to contaminants on their surface. This stress arises from the additional effort required to digest inert material and maintain physiological homeostasis [114,115]. Another hypothesis proposes that MPs may cause microscale abrasions in the internal tissues of organisms, rendering them more

vulnerable to other contaminants in the aquatic environment [115,116]. Metabolic rates can also be impacted by adverse effects from MPs, arising from their ability to hinder oxygen uptake [89], which can ultimately affect swimming behavior.

The interplays of experimental parameters and measured endpoints, uptake quantity, and particle size showed the strongest correlation. Although the strength of the relationship between locomotion, growth, and uptake was mainly weak, statistically significant *p*-values indicated that the association between the variables was unlikely to be coincidental. Consequently, uptake may have led to TDM, thigmotaxis, and velocity alterations. Given that behavior acts as a pivotal connector between biological scales, bridging subcellular processes measurable in laboratories with ecological reactions to contaminants in natural settings, the interaction of MNPs with temperature has the potential to influence behaviors such as feeding, predator avoidance, and reproductive success. Additional investigations are necessary to explore the indirect consequences of MNPs exposure, especially in the context of climate change and further abiotic factors.

It is important to recognize that our study possesses certain limitations. One notable limitation pertains to the size, shape, and polymer of the particles used, as well as their concentrations. We recognize that the plastics employed may not reflect the diverse array of materials found in natural aquatic systems, where various types and sizes of plastics coexist at varying concentrations. Detecting NPs in the field remains challenging; however, future studies could explore strategies to do so and evaluate their impact on aquatic systems. In order to establish a robust foundation for risk assessment, future experimental methodologies should not only consider the ability to differentiate between the impacts of food scarcity and particle toxicity, but also ascertain whether MNPs elicit effects distinct from those induced by naturally occurring particles [117]. Knowledge gaps underscore the need for further research encompassing a broader spectrum of plastic characteristics and environmental conditions to provide a more comprehensive understanding of the complex interactions between plastics and aquatic ecosystems. It is imperative to conduct additional investigations on the role of the food chain as a conduit for the distribution of plastic debris, particularly MPs, among aquatic organisms spanning from the primary to higher trophic levels [118]. The investigation of excretion and uptake dynamics over time was not within the scope of this study; however, these aspects represent significant knowledge gaps warranting exploration in future research endeavors. Future studies should also investigate the combined effects of MNPs and temperature on oxidative stress. Exposures of HA to polyethylene terephthalate were shown to influence oxidative stress indicators (Superoxide dismutase, Malondialdehyde, and Glutathione S-transferase), enzymes, which are crucial components of the primary antioxidant defense system against reactive oxygen species [119]. Despite these limitations, our study offers valuable insights into the potential impacts of rising temperatures on plastic pollution dynamics and highlights avenues for future investigations to bridge the gap between laboratory experimentation and real-world ecological contexts. Building upon our findings, future investigations should explore the interactive effects of temperature and plastic pollution on broader ecological processes, such as species interactions, nutrient cycling, and ecosystem functioning. Furthermore, the insights gleaned from our study could inform the development of innovative mitigation strategies and policy interventions geared towards curbing plastic pollution and safeguarding vulnerable aquatic ecosystems. Interdisciplinary approaches, and advances in technology and analytical techniques could be used to find solutions for mitigating the impacts of plastic pollution while following sustainable management practices.

5. Conclusions

This study illustrates how variations in environmental temperature can modify the effects of micro- and nano-sized PS beads. Our results show that the combination of PS particles and higher temperatures can cause a risk to HA. Elevated temperatures augmented particle uptake in treatments involving 500 nm particles, whereas growth was diminished in treatments with 1000 nm particles. Swimming behavior exhibited disparities across particle

sizes, while survival rates decreased for both particle sizes at 27 °C. However, understanding how plastic particle effects intertwine with abiotic factors like temperature remains limited to this day. Employing model organisms such as HA, prominent amphipods within aquatic food webs can facilitate in assessing these impacts and identifying potential risks of MNPs such as polystyrene. We also aimed to explore the impact of particle uptake on the behavior of HA, presently lacking in the MNPs literature. Our results highlight the significant influence of exposure on behavioral endpoints, thus improving our ability to assess risk through the identification of indicators. This toolkit can aid in determining the risks associated with plastics by employing a USEPA epibenthic model.

Supplementary Materials: The following supporting information can be downloaded at: <https://www.mdpi.com/article/10.3390/w16101360/s1>, Figure S1. Spectral absorption and emission graph of polystyrene beads. Blue fluorescent beads with a mean diameter of 519 and 1294 nm were ordered from Applied Microspheres GmbH (formerly BS-Partikel GmbH, Mainz, Germany) at a concentration of 5% m/m (Surface: not-modified polystyrol, no surface functionalization, sulfonic acid end group). Table S1. Tested polystyrene concentrations in the range finder study (*). “Conc. 5” was used in the main exposure study. Figure S2. Temperature logger data from each climate chamber set to 21, 24, and 27 °C during the 96 h exposure starting on 10/21. Table S2. Water parameters were measured via YSI during the 96 h exposure of *H. azteca* to polystyrene particles at three temperatures (21 °C, 24 °C, 27 °C). The three temperatures were regulated in climate chambers (Ch1-3). Table S3. Correlation between *H. azteca* behavioral parameters (either TDM or thigmotaxis) and the polystyrene particle treatment (control, 500 nm, 1000 nm), or the temperature (21 °C, 24 °C, 27 °C) in the dark and light period. Spearman correlation matrix: * $p < 0.05$ are marked in red. Figure S3. Uptake across particle (500 nm or 1000 nm sized polystyrene particles) and temperature treatments of pooled *H. azteca* (N = 14–19) by ranking: 1 = minor fluorescence (only stomach and mouth parts), 2 = fluorescence additionally in parts of the guts, 3 = fluorescence in the majority of the gut. Figure S4. Examples of confocal images for quantifying fluorescent 500 nm or 1000 nm polystyrene particle uptake by *H. azteca* at 24 °C: Maximal intensity of z-stack layers. Figure S5. Correlation between PS uptake and endpoints: Spearman correlation (r_s values) between *H. azteca* uptake and further endpoints. Strongest correlation: Uptake vs. particle treatment ($r_s = 0.67$; $p < 0.001$). The r values of 0–0.19 are commonly regarded as very weak, 0.2–0.39 as weak, 0.40–0.59 as moderate, 0.6–0.79 as strong and 0.8–1 as very strong.

Author Contributions: Conceptualization, F.B., S.M.B., R.E.C. and J.G.; methodology, investigation, formal analysis, data curation, writing, F.B.; review, editing and investigation, F.B., S.M.B., R.E.C. and J.G.; supervision, project administration, funding acquisition, R.E.C. and J.G. All authors have read and agreed to the published version of the manuscript.

Funding: Funding for Felix Biefel was provided by the Bayerische Forschungsstiftung (DOK-181-19, Geist). The ideas presented in this publication are those solely of the authors and do not necessarily reflect the opinions of the granting agency.

Data Availability Statement: The data presented in this study are available upon request to Felix Biefel (felix.biefel@tum.de).

Acknowledgments: The authors would like to thank Erin Lamphear and Amelie Segarra for their assistance on behavioral assay analysis and advice on statistical approaches. The confocal microscopic analyses would not have been possible without the help of Ingrid Brust-Mascher (Advanced Imaging Facility of UC Davis).

Conflicts of Interest: The authors declare that they have no known competing financial interests or personal relationships that could have appeared to influence the work reported in this paper.

References

1. Baekeland, L.H. The Synthesis, Constitution, and Uses of Bakelite. *Ind. Eng. Chem.* **1909**, *1*, 149–161. [CrossRef]
2. OECD Global Plastics Outlook. *Global Plastics Outlook*; OECD: Paris, France, 2022. [CrossRef]
3. Dioses-Salinas, D.C.; Pizarro-Ortega, C.I.; De-la-Torre, G.E. A Methodological Approach of the Current Literature on Microplastic Contamination in Terrestrial Environments: Current Knowledge and Baseline Considerations. *Sci. Total Environ.* **2020**, *730*, 139164. [CrossRef] [PubMed]

4. Feng, S.; Lu, H.; Tian, P.; Xue, Y.; Lu, J.; Tang, M.; Feng, W. Analysis of Microplastics in a Remote Region of the Tibetan Plateau: Implications for Natural Environmental Response to Human Activities. *Sci. Total Environ.* **2020**, *739*, 140087. [[CrossRef](#)] [[PubMed](#)]
5. da Costa, J.P.; Santos, P.S.M.; Duarte, A.C.; Rocha-Santos, T. (Nano)Plastics in the Environment—Sources, Fates and Effects. *Sci. Total Environ.* **2016**, *566–567*, 15–26. [[CrossRef](#)] [[PubMed](#)]
6. Battisti, C.; Fanelli, G.; Gallitelli, L.; Scalici, M. Dunal Plants as Sink for Anthropogenic Marine Litter: The Entrapping Role of *Salsola kali* L. (1753) in a Mediterranean Remote Beach (Sardinia, Italy). *Mar. Pollut. Bull.* **2023**, *192*, 115033. [[CrossRef](#)] [[PubMed](#)]
7. Lee, C.H.; Fang, J.K.H. Effects of Temperature and Particle Concentration on Aggregation of Nanoplastics in Freshwater and Seawater. *Sci. Total Environ.* **2022**, *817*, 152562. [[CrossRef](#)]
8. Felicia Coleman, B.; S Wehle, D.H. Plastic Pollution: A Worldwide Oceanic Problem. *Parks* **1984**, *9*, 9–12.
9. Battisti, C.; Gallitelli, L.; Vanadia, S.; Scalici, M. General Macro-Litter as a Proxy for Fishing Lines, Hooks and Nets Entrapping Beach-Nesting Birds: Implications for Clean-Ups. *Mar. Pollut. Bull.* **2023**, *186*, 114502. [[CrossRef](#)]
10. Koltzenburg, S.; Maskos, M.; Nuyken, O. *Polymer Chemistry*; Springer: Berlin/Heidelberg, Germany, 2017; pp. 1–584. [[CrossRef](#)]
11. Worm, B.; Lotze, H.K.; Jubinville, I.; Wilcox, C.; Jambeck, J. Plastic as a Persistent Marine Pollutant. *Annu. Rev. Environ. Resour.* **2017**, *42*, 1–26. [[CrossRef](#)]
12. Klein, S.; Dimzon, I.K.; Eubeler, J.; Knepper, T.P. Analysis, Occurrence, and Degradation of Microplastics in the Aqueous Environment. In *Handbook of Environmental Chemistry*; Springer: Berlin/Heidelberg, Germany, 2018; Volume 58, pp. 51–67.
13. Liu, F.; Rasmussen, L.A.; Klemmensen, N.D.R.; Zhao, G.; Nielsen, R.; Vianello, A.; Rist, S.; Vollertsen, J. Shapes of Hyperspectral Imaged Microplastics. *Environ. Sci. Technol.* **2023**, *57*, 12431–12441. [[CrossRef](#)] [[PubMed](#)]
14. Wright, S.L.; Thompson, R.C.; Galloway, T.S. The Physical Impacts of Microplastics on Marine Organisms: A Review. *Environ. Pollut.* **2013**, *178*, 483–492. [[CrossRef](#)]
15. Anbumani, S.; Kakkar, P. Ecotoxicological Effects of Microplastics on Biota: A Review. *Environ. Sci. Pollut. Res.* **2018**, *25*, 14373–14396. [[CrossRef](#)] [[PubMed](#)]
16. Lehtiniemi, M.; Hartikainen, S.; Näkki, P.; Engström-Öst, J.; Koistinen, A.; Setälä, O. Size Matters More than Shape: Ingestion of Primary and Secondary Microplastics by Small Predators. *Food Webs* **2018**, *17*, e00097. [[CrossRef](#)]
17. Doyle, D.; Sundh, H.; Almröth, B.C. Microplastic Exposure in Aquatic Invertebrates Can Cause Significant Negative Effects Compared to Natural Particles—A Meta-Analysis. *Environ. Pollut.* **2022**, *315*, 120434. [[CrossRef](#)] [[PubMed](#)]
18. Biefel, F.; Geist, J.; Cannon, R.; Pollution, B.H.-E. *Interactive Effects between Water Temperature, Microparticle Compositions, and Fiber Types on the Marine Keystone Species *Americamysis Bahía**; Elsevier: Amsterdam, The Netherlands, 2024.
19. Redondo-Hasselerharm, P.E.; Falahudin, D.; Peeters, E.T.H.M.; Koelmans, A.A. Microplastic Effect Thresholds for Freshwater Benthic Macroinvertebrates. *Environ. Sci. Technol.* **2018**, *52*, 2278–2286. [[CrossRef](#)] [[PubMed](#)]
20. Magester, S.; Barcelona, A.; Colomer, J.; Serra, T. Vertical Distribution of Microplastics in Water Bodies Causes Sublethal Effects and Changes in *Daphnia Magna* Swimming Behaviour. *Ecotoxicol. Environ. Saf.* **2021**, *228*, 113001. [[CrossRef](#)] [[PubMed](#)]
21. Ruthsatz, K.; Schwarz, A.; Gomez-Mestre, I.; Meyer, R.; Domscheit, M.; Bartels, F.; Schaeffer, S.M.; Engelkes, K. Life in Plastic, It's Not Fantastic: Sublethal Effects of Polyethylene Microplastics Ingestion throughout Amphibian Metamorphosis. *Sci. Total Environ.* **2023**, *885*, 163779. [[CrossRef](#)] [[PubMed](#)]
22. Greven, A.C.; Merk, T.; Karagöz, F.; Mohr, K.; Klapper, M.; Jovanović, B.; Palić, D. Polycarbonate and Polystyrene Nanoplastic Particles Act as Stressors to the Innate Immune System of Fathead Minnow (*Pimephales promelas*). *Environ. Toxicol. Chem.* **2016**, *35*, 3093–3100. [[CrossRef](#)] [[PubMed](#)]
23. Lu, Y.; Zhang, Y.; Deng, Y.; Jiang, W.; Zhao, Y.; Geng, J.; Ding, L.; Ren, H. Uptake and Accumulation of Polystyrene Microplastics in Zebrafish (*Danio rerio*) and Toxic Effects in Liver. *Environ. Sci. Technol.* **2016**, *50*, 4054–4060. [[CrossRef](#)] [[PubMed](#)]
24. Cunningham, B.; Harper, B.; Brander, S.; Harper, S. Toxicity of Micro and Nano Tire Particles and Leachate for Model Freshwater Organisms. *J. Hazard. Mater.* **2022**, *429*, 128319. [[CrossRef](#)] [[PubMed](#)]
25. Ziajahromi, S.; Kumar, A.; Neale, P.A.; Leusch, F.D.L. Environmentally Relevant Concentrations of Polyethylene Microplastics Negatively Impact the Survival, Growth and Emergence of Sediment-Dwelling Invertebrates. *Environ. Pollut.* **2018**, *236*, 425–431. [[CrossRef](#)] [[PubMed](#)]
26. Koelmans, A.A.; Besseling, E.; Foekema, E.; Kooi, M.; Mintenig, S.; Ossendorp, B.C.; Redondo-Hasselerharm, P.E.; Verschoor, A.; Van Wezel, A.P.; Scheffer, M. Risks of Plastic Debris: Unravelling Fact, Opinion, Perception, and Belief. *Environ. Sci. Technol.* **2017**, *51*, 11513–11519. [[CrossRef](#)] [[PubMed](#)]
27. Triebkorn, R.; Braunbeck, T.; Grummt, T.; Hanslik, L.; Huppertsberg, S.; Jekel, M.; Knepper, T.P.; Kraus, S.; Müller, Y.K.; Pittroff, M.; et al. Relevance of Nano- and Microplastics for Freshwater Ecosystems: A Critical Review. *TrAC Trends Anal. Chem.* **2019**, *110*, 375–392. [[CrossRef](#)]
28. Keerthika, K.; Padmavathy, P.; Rani, V.; Jeyashakila, R.; Aanand, S.; Kutty, R.; Tamilselvan, R.; Subash, P. Microplastics Accumulation in Pelagic and Benthic Species along the Thoothukudi Coast, South Tamil Nadu, India. *Mar. Pollut. Bull.* **2023**, *189*, 114735. [[CrossRef](#)]
29. Zavala-Alarcón, F.L.; Huchin-Mian, J.P.; González-Muñoz, M.D.P.; Kozak, E.R. In Situ Microplastic Ingestion by Neritic Zooplankton of the Central Mexican Pacific. *Environ. Pollut.* **2023**, *319*, 120994. [[CrossRef](#)] [[PubMed](#)]
30. McIlwraith, H.K.; Kim, J.; Helm, P.; Bhavsar, S.P.; Metzger, J.S.; Rochman, C.M. Evidence of Microplastic Translocation in Wild-Caught Fish and Implications for Microplastic Accumulation Dynamics in Food Webs. *ACS Publ.* **2021**, *55*, 12372–12382. [[CrossRef](#)] [[PubMed](#)]

31. Liu, Y.; Qiu, X.; Xu, X.; Takai, Y.; Ogawa, H.; Shimasaki, Y.; Oshima, Y. Uptake and Depuration Kinetics of Microplastics with Different Polymer Types and Particle Sizes in Japanese Medaka (*Oryzias latipes*). *Ecotoxicol. Environ. Saf.* **2021**, *212*, 112007. [CrossRef]
32. Holomuzki, J.R.; Feminella, J.W.; Power, M.E. Biotic Interactions in Freshwater Benthic Habitats. *J. N. Am. Benthol. Soc.* **2010**, *29*, 220–244. [CrossRef]
33. Yang, L.; Zhang, Y.; Kang, S.; Wang, Z.; Wu, C. Microplastics in Freshwater Sediment: A Review on Methods, Occurrence, and Sources. *Sci. Total Environ.* **2021**, *754*, 141948. [CrossRef] [PubMed]
34. Melo, S.L.R.; Nipper, M. Sediment Toxicity Tests Using the Burrowing Amphipod *Tiburonella Viscana* (Amphipoda: Platyschnopidae). *Ecotoxicol. Environ. Saf.* **2007**, *66*, 412–420. [CrossRef] [PubMed]
35. Glazier, D.S. Amphipoda. In *Reference Module in Earth Systems and Environmental Sciences*; Elsevier: Amsterdam, The Netherlands, 2014. [CrossRef]
36. Péry, A.R.R.; Dargelos, S.; Quéau, H.; Garric, J. Preparatory Work to Propose Water-Only Tests with the Amphipod *Hyalella Azteca*: Comparison with Sediment Toxicity Tests. *Bull. Environ. Contam. Toxicol.* **2005**, *75*, 617–622. [CrossRef] [PubMed]
37. Javidmehr, A.; Kass, P.H.; Deanovic, L.A.; Connon, R.E.; Werner, I. 10-Day Survival of *Hyalella Azteca* as a Function of Water Quality Parameters. *Ecotoxicol. Environ. Saf.* **2015**, *115*, 250–256. [CrossRef] [PubMed]
38. Growth, Development and Reproduction of *Hyalella azteca* (Saussure, 1858) in Laboratory Culture on JSTOR. Available online: <https://www.jstor.org/stable/20106425> (accessed on 1 May 2024).
39. Khan, F.R.; Halle, L.L.; Palmqvist, A. Acute and Long-Term Toxicity of Micronized Car Tire Wear Particles to *Hyalella Azteca*. *Aquat. Toxicol.* **2019**, *213*, 105216. [CrossRef] [PubMed]
40. Carpenter, E.J.; Anderson, S.J.; Harvey, G.R.; Miklas, H.P.; Peck, B.B. Polystyrene Spherules in Coastal Waters. *Science* **1972**, *178*, 749–750. [CrossRef]
41. Koelmans, A.A.; Bakir, A.; Burton, G.A.; Janssen, C.R. Microplastic as a Vector for Chemicals in the Aquatic Environment: Critical Review and Model-Supported Reinterpretation of Empirical Studies. *Environ. Sci. Technol.* **2016**, *50*, 3315–3326. [CrossRef] [PubMed]
42. Alimi, O.S.; Farner Budarz, J.; Hernandez, L.M.; Tufenkji, N. Microplastics and Nanoplastics in Aquatic Environments: Aggregation, Deposition, and Enhanced Contaminant Transport. *Environ. Sci. Technol.* **2017**, *52*, 1704–1724. [CrossRef] [PubMed]
43. Ho, B.T.; Roberts, T.K.; Lucas, S. An Overview on Biodegradation of Polystyrene and Modified Polystyrene: The Microbial Approach. *Crit. Rev. Biotechnol.* **2018**, *38*, 308–320. [CrossRef]
44. Rani-Borges, B.; Queiroz, L.G.; Achilles Prado, C.C.; de Melo, E.C.; de Moraes, B.R.; Ando, R.A.; de Paiva, T.C.B.; Pompeo, M.M. Expressive Biofragmentation of Polystyrene Microplastics by the Amphipod *Hyalella Azteca*. *SSRN Electron. J.* **2022**. [CrossRef]
45. Rani-Borges, B.; Queiroz, L.G.; Prado, C.C.A.; de Melo, E.C.; de Moraes, B.R.; Ando, R.A.; de Paiva, T.C.B.; Pompêo, M. Exposure of the Amphipod *Hyalella Azteca* to Microplastics. A Study on Subtoxic Responses and Particle Biofragmentation. *Aquat. Toxicol.* **2023**, *258*, 106516. [CrossRef]
46. Verslycke, T.; Janssen, C.R. Effects of a Changing Abiotic Environment on the Energy Metabolism in the Estuarine Mysid Shrimp *Neomysis Integer* (Crustacea: Mysidacea). *J. Exp. Mar. Biol. Ecol.* **2002**, *279*, 61–72. [CrossRef]
47. Reyes, B.A.; Pendergast, J.S.; Yamazaki, S. Mammalian Peripheral Circadian Oscillators Are Temperature Compensated. *J. Biol. Rhythm.* **2008**, *23*, 95–98. [CrossRef] [PubMed]
48. Han, X.; Zheng, Y.; Dai, C.; Duan, H.; Gao, M.; Ali, M.R.; Sui, L. Effect of Polystyrene Microplastics and Temperature on Growth, Intestinal Histology and Immune Responses of Brine Shrimp *Artemia Franciscana*. *J. Oceanol. Limnol.* **2021**, *39*, 979–988. [CrossRef]
49. Na, J.; Song, J.; Jung, J. Elevated Temperature Enhanced Lethal and Sublethal Acute Toxicity of Polyethylene Microplastic Fragments in *Daphnia Magna*. *Environ. Toxicol. Pharmacol.* **2023**, *102*, 104212. [CrossRef] [PubMed]
50. Mundy, P.C.; Hartz, K.E.H.; Fulton, C.A.; Lydy, M.J.; Brander, S.M.; Hung, T.-C.; Fanguie, N.A.; Connon, R.E. Exposure to Permethrin or Chlorpyrifos Causes Differential Dose- and Time-Dependent Behavioral Effects at Early Larval Stages of an Endangered Teleost Species. *Endanger. Species Res.* **2021**, *44*, 89–103. [CrossRef] [PubMed]
51. Segarra, A.; Mauduit, F.; Amer, N.R.; Biefel, F.; Hladik, M.L.; Connon, R.E.; Brander, S.M. Salinity Changes the Dynamics of Pyrethroid Toxicity in Terms of Behavioral Effects on Newly Hatched Delta Smelt Larvae. *Toxics* **2021**, *9*, 40. [CrossRef] [PubMed]
52. Hasenbein, S.; Lawler, S.P.; Geist, J.; Connon, R.E. The Use of Growth and Behavioral Endpoints to Assess the Effects of Pesticide Mixtures upon Aquatic Organisms. *Ecotoxicology* **2015**, *24*, 746–759. [CrossRef] [PubMed]
53. Kristofco, L.A.; Cruz, L.C.; Haddad, S.P.; Behra, M.L.; Chambliss, C.K.; Brooks, B.W. Age Matters: Developmental Stage of Danio Rerio Larvae Influences Photomotor Response Thresholds to Diazinon or Diphenhydramine. *Aquat. Toxicol.* **2016**, *170*, 344–354. [CrossRef]
54. Evans, H.L. Neurotoxicity Expressed in Naturally Occurring Behavior. In *Neurobehavioral Toxicity: Analysis and Interpretation*; CRC Press: Boca Raton, FL, USA, 1994; pp. 111–135.
55. Bridges, C.M. Tadpole Swimming Performance and Activity Affected by Acute Exposure to Sublethal Levels of Carbaryl. *Environ. Toxicol. Chem.* **1997**, *16*, 1935–1939. [CrossRef]
56. Grue, C.; Gardner, S.; Gibert, P.L.; Dell Omo, G. *Behavioural Ecotoxicology*; Wiley: Hoboken, NJ, USA, 2002.
57. Jacob, H.; Besson, M.; Swarzenski, P.W.; Lecchini, D.; Metian, M. Effects of Virgin Micro- and Nanoplastics on Fish: Trends, Meta-Analysis, and Perspectives. *Environ. Sci. Technol.* **2020**, *54*, 4733–4745. [CrossRef]

58. Wang, X.; Liu, L.; Zheng, H.; Wang, M.; Fu, Y.; Luo, X.; Li, F.; Wang, Z. Polystyrene Microplastics Impaired the Feeding and Swimming Behavior of Mysid Shrimp *Neomysis Japonica*. *Mar. Pollut. Bull.* **2020**, *150*, 110660. [CrossRef]
59. Britt, E. Erickson Getting a Grip on Microplastics' Risks. *CEN Glob. Enterp.* **2022**, *100*, 20–25. [CrossRef]
60. Qiao, R.; Mortimer, M.; Richter, J.; Rani-Borges, B.; Yu, Z.; Heinlaan, M.; Lin, S.; Ivask, A. Hazard of Polystyrene Micro-and Nanospheres to Selected Aquatic and Terrestrial Organisms. *Sci. Total Environ.* **2022**, *853*, 158560. [CrossRef] [PubMed]
61. US EPA. *Methods for Measuring the Acute Toxicity of Effluents and Receiving Waters to Freshwater and Marine Organisms*, 5th ed.; US EPA: Washington, DC, USA, 2002; p. EPA-821-R-02-012.
62. US EPA. Ecological Effects Test Guidelines OPPTS 850.1020 Gammarid Acute Toxicity Test. Available online: https://scholar.google.com/scholar_lookup?title=Ecological%20Effects%20Test%20Guidelines%20OPPTS%20850.1020%20Gammarid%20Acute%20Toxicity%20Test&publication_year=1996&author=USEPA (accessed on 25 February 2024).
63. US EPA. *Methods for Measuring the Toxicity and Bioaccumulation of Sediment-Associated Contaminants with Freshwater Invertebrates*; Duluth, M.N., Verschuere, K., Eds.; US EPA: Washington, DC, USA, 2000; Volume 58, pp. 255–267.
64. Götz, A.; Imhof, H.K.; Geist, J.; Beggel, S. Moving Toward Standardized Toxicity Testing Procedures with Particulates by Dietary Exposure of Gammarids. *Environ. Toxicol. Chem.* **2021**, *40*, 1463–1476. [CrossRef] [PubMed]
65. Götz, A.; Beggel, S.; Geist, J. Dietary Exposure to Four Sizes of Spherical Polystyrene, Polylactide and Silica Nanoparticles Does Not Affect Mortality, Behaviour, Feeding and Energy Assimilation of *Gammarus Roeseli*. *Ecotoxicol. Environ. Saf.* **2022**, *238*, 113581. [CrossRef] [PubMed]
66. Besseling, E.; Redondo-Hasselerharm, P.; Foekema, E.M.; Koelmans, A.A. Quantifying Ecological Risks of Aquatic Micro- and Nanoplastic. *Crit. Rev. Environ. Sci. Technol.* **2019**, *49*, 32–80. [CrossRef]
67. Lasee, S.; Mauricio, J.; Thompson, W.A.; Karnjanapiboonwong, A.; Kasumba, J.; Subbiah, S.; Morse, A.N.; Anderson, T.A. Microplastics in a Freshwater Environment Receiving Treated Wastewater Effluent. *Integr. Environ. Assess. Manag.* **2017**, *13*, 528–532. [CrossRef] [PubMed]
68. Frias, J.P.G.L.; Otero, V.; Sobral, P. Evidence of Microplastics in Samples of Zooplankton from Portuguese Coastal Waters. *Mar. Environ. Res.* **2014**, *95*, 89–95. [CrossRef] [PubMed]
69. Isobe, A.; Uchida, K.; Tokai, T.; Iwasaki, S. East Asian Seas: A Hot Spot of Pelagic Microplastics. *Mar. Pollut. Bull.* **2015**, *101*, 618–623. [CrossRef] [PubMed]
70. Beiras, R.; Schönemann, A.M. Currently Monitored Microplastics Pose Negligible Ecological Risk to the Global Ocean. *Sci. Rep.* **2020**, *10*, 22281. [CrossRef] [PubMed]
71. Su, L.; Xue, Y.; Li, L.; Yang, D.; Kolandhasamy, P.; Li, D.; Shi, H. Microplastics in Taihu Lake, China. *Environ. Pollut.* **2016**, *216*, 711–719. [CrossRef] [PubMed]
72. Mao, Y.; Ai, H.; Chen, Y.; Zhang, Z.; Zeng, P.; Kang, L.; Li, W.; Gu, W.; He, Q.; Li, H. Phytoplankton Response to Polystyrene Microplastics: Perspective from an Entire Growth Period. *Chemosphere* **2018**, *208*, 59–68. [CrossRef] [PubMed]
73. Liu, L.; Song, J.; Zhang, M.; Jiang, W. Aggregation and Deposition Kinetics of Polystyrene Microplastics and Nanoplastics in Aquatic Environment. *Bull. Environ. Contam. Toxicol.* **2021**, *107*, 741–747. [CrossRef] [PubMed]
74. Wilhelm, F.M.; Lasenby, D.C. Seasonal Trends in the Head Capsule Length and Body Length/Weight Relationships of Two Amphipod Species. *Crustaceana* **1998**, *71*, 399–410. [CrossRef]
75. Schindelin, J.; Arganda-Carreras, I.; Frise, E.; Kaynig, V.; Longair, M.; Pietzsch, T.; Preibisch, S.; Rueden, C.; Saalfeld, S.; Schmid, B.; et al. Fiji: An Open-Source Platform for Biological-Image Analysis. *Nat. Methods* **2012**, *9*, 676–682. [CrossRef] [PubMed]
76. Schneider, C.A.; Rasband, W.S.; Eliceiri, K.W. NIH Image to ImageJ: 25 Years of Image Analysis. *Nat. Methods* **2012**, *9*, 671–675. [CrossRef] [PubMed]
77. Siddiqui, S.; Hutton, S.J.; Dickens, J.M.; Pedersen, E.I.; Harper, S.L.; Brander, S.M. Natural and Synthetic Microfibers Alter Growth and Behavior in Early Life Stages of Estuarine Organisms. *Front. Mar. Sci.* **2023**, *9*, 991650. [CrossRef]
78. Siddiqui, S.; Dickens, J.M.; Cunningham, B.E.; Hutton, S.J.; Pedersen, E.I.; Harper, B.; Harper, S.; Brander, S.M. Internalization, Reduced Growth, and Behavioral Effects Following Exposure to Micro and Nano Tire Particles in Two Estuarine Indicator Species. *Chemosphere* **2022**, *296*, 133934. [CrossRef]
79. Au, S.Y.; Bruce, T.F.; Bridges, W.C.; Klaine, S.J. Responses of *Hyalella Azteca* to Acute and Chronic Microplastic Exposures. *Environ. Toxicol. Chem.* **2015**, *34*, 2564–2572. [CrossRef]
80. Mattsson, K.; Adolfsson, K.; Ekvall, M.T.; Borgström, M.T.; Linse, S.; Hansson, L.A.; Cedervall, T.; Prinz, C.N. Translocation of 40 Nm Diameter Nanowires through the Intestinal Epithelium of *Daphnia Magna*. *Nanotoxicology* **2016**, *10*, 1160–1167. [CrossRef] [PubMed]
81. Li, L.; Luo, Y.; Peijnenburg, W.J.G.M.; Li, R.; Yang, J.; Zhou, Q. Confocal Measurement of Microplastics Uptake by Plants. *MethodsX* **2020**, *7*, 100750. [CrossRef]
82. Ma, C.; Li, L.; Chen, Q.; Lee, J.S.; Gong, J.; Shi, H. Application of Internal Persistent Fluorescent Fibers in Tracking Microplastics in Vivo Processes in Aquatic Organisms. *J. Hazard. Mater.* **2021**, *401*, 123336. [CrossRef] [PubMed]
83. Kuehr, S.; Kaegi, R.; Maletzki, D.; Schleichriem, C. Testing the Bioaccumulation Potential of Manufactured Nanomaterials in the Freshwater Amphipod *Hyalella Azteca*. *Chemosphere* **2021**, *263*, 127961. [CrossRef] [PubMed]
84. Kuehr, S.; Diehle, N.; Kaegi, R.; Schleichriem, C. Ingestion of Bivalve Droppings by Benthic Invertebrates May Lead to the Transfer of Nanomaterials in the Aquatic Food Chain. *Environ. Sci. Eur.* **2021**, *33*, 35. [CrossRef]

85. Kuehr, S.; Windisch, H.; Schleichtrien, C.; Leon, G.; Gasparini, G.; Gimeno, S. Are Fragrance Encapsulates Taken Up by Aquatic and Terrestrial Invertebrate Species? *Environ. Toxicol. Chem.* **2022**, *41*, 931–943. [[CrossRef](#)] [[PubMed](#)]
86. Machin, D.; Cheung, Y.B.; Parmar, M.K. *Survival Analysis: A Practical Approach*, 2nd ed.; Wiley: Hoboken, NJ, USA, 2006; pp. 1–266. [[CrossRef](#)]
87. Vega-Garcia, D.; Brito-Parada, P.R.; Cilliers, J.J. Optimising Small Hydrocyclone Design Using 3D Printing and CFD Simulations. *Chem. Eng. J.* **2018**, *350*, 653–659. [[CrossRef](#)]
88. Ogonowski, M.; Schür, C.; Jarsén, Å.; Gorokhova, E. The Effects of Natural and Anthropogenic Microparticles on Individual Fitness in *Daphnia Magna*. *PLoS ONE* **2016**, *11*, e0155063. [[CrossRef](#)] [[PubMed](#)]
89. Rist, S.E.; Assidqi, K.; Zamani, N.P.; Appel, D.; Perschke, M.; Huhn, M.; Lenz, M. Suspended Micro-Sized PVC Particles Impair the Performance and Decrease Survival in the Asian Green Mussel *Perna Viridis*. *Mar. Pollut. Bull.* **2016**, *111*, 213–220. [[CrossRef](#)] [[PubMed](#)]
90. Wen, B.; Zhang, N.; Jin, S.R.; Chen, Z.Z.; Gao, J.Z.; Liu, Y.; Liu, H.P.; Xu, Z. Microplastics Have a More Profound Impact than Elevated Temperatures on the Predatory Performance, Digestion and Energy Metabolism of an Amazonian Cichlid. *Aquat. Toxicol.* **2018**, *195*, 67–76. [[CrossRef](#)]
91. Zhou, N.; Wang, Z.; Yang, L.; Zhou, W.; Qin, Z.; Zhang, H. Size-Dependent Toxicological Effects of Polystyrene Microplastics in the Shrimp *Litopenaeus Vannamei* Using a Histomorphology, Microbiome, and Metabolic Approach. *Environ. Pollut.* **2023**, *316*, 120635. [[CrossRef](#)] [[PubMed](#)]
92. Blarer, P.; Burkhardt-Holm, P. Microplastics Affect Assimilation Efficiency in the Freshwater Amphipod *Gammarus Fossarum*. *Environ. Sci. Pollut. Res.* **2016**, *23*, 23522–23532. [[CrossRef](#)]
93. Straub, S.; Hirsch, P.E.; Burkhardt-Holm, P. Biodegradable and Petroleum-Based Microplastics Do Not Differ in Their Ingestion and Excretion but in Their Biological Effects in a Freshwater Invertebrate *Gammarus Fossarum*. *Int. J. Environ. Res. Public Health* **2017**, *14*, 774. [[CrossRef](#)] [[PubMed](#)]
94. Kratina, P.; Watts, T.J.; Green, D.S.; Kordas, R.L.; O’Gorman, E.J. Interactive Effects of Warming and Microplastics on Metabolism but Not Feeding Rates of a Key Freshwater Detritivore. *Environ. Pollut.* **2019**, *255*, 113259. [[CrossRef](#)] [[PubMed](#)]
95. Molenaar, R.; Chatterjee, S.; Kamphuis, B.; Segers-Nolten, I.M.J.; Claessens, M.M.A.E.; Blum, C. Nanoplastic Sizes and Numbers: Quantification by Single Particle Tracking. *Environ. Sci. Nano* **2021**, *8*, 723–730. [[CrossRef](#)]
96. Gillooly, J.F.; Brown, J.H.; West, G.B.; Savage, V.M.; Charnov, E.L. Effects of Size and Temperature on Metabolic Rate. *Science* **2001**, *293*, 2248–2251. [[CrossRef](#)] [[PubMed](#)]
97. Ohlberger, J. Climate Warming and Ectotherm Body Size—From Individual Physiology to Community Ecology. *Funct. Ecol.* **2013**, *27*, 991–1001. [[CrossRef](#)]
98. Brown, J.H.; Gillooly, J.F.; Allen, A.P.; Savage, V.M.; West, G.B. Toward a metabolic theory of ecology. *Ecology* **2004**, *85*, 1771–1789. [[CrossRef](#)]
99. Rall, B.C.; Brose, U.; Hartvig, M.; Kalinkat, G.; Schwarzmüller, F.; Vucic-Pestic, O.; Petchey, O.L. Universal Temperature and Body-Mass Scaling of Feeding Rates. *Philos. Trans. R. Soc. B Biol. Sci.* **2012**, *367*, 2923–2934. [[CrossRef](#)] [[PubMed](#)]
100. Schmitz, E.H.; Scherrey, P.M. Digestive Anatomy of *Halella Azteca* (Crustacea, Amphipoda). *J. Morphol.* **1983**, *175*, 91–100. [[CrossRef](#)] [[PubMed](#)]
101. Li, H.; Chen, H.; Wang, J.; Li, J.; Liu, S.; Tu, J.; Chen, Y.; Zong, Y.; Zhang, P.; Wang, Z.; et al. Influence of Microplastics on the Growth and the Intestinal Microbiota Composition of Brine Shrimp. *Front. Microbiol.* **2021**, *12*, 717272. [[CrossRef](#)] [[PubMed](#)]
102. van Pomeran, M.; Brun, N.R.; Peijnenburg, W.J.G.M.; Vijver, M.G. Exploring Uptake and Biodistribution of Polystyrene (Nano)Particles in Zebrafish Embryos at Different Developmental Stages. *Aquat. Toxicol.* **2017**, *190*, 40–45. [[CrossRef](#)] [[PubMed](#)]
103. Tenuta, T.; Monopoli, M.P.; Kim, J.; Salvati, A.; Dawson, K.A. Elution of Labile Fluorescent Dye from Nanoparticles during Biological Use. *PLoS ONE* **2011**, *6*, 25556. [[CrossRef](#)] [[PubMed](#)]
104. Schür, C.; Rist, S.; Baun, A.; Mayer, P.; Hartmann, N.B.; Wagner, M. When Fluorescence Is Not a Particle: The Tissue Translocation of Microplastics in *Daphnia Magna* Seems an Artifact. *Environ. Toxicol. Chem.* **2019**, *38*, 1495–1503. [[CrossRef](#)] [[PubMed](#)]
105. Wang, F.; Wong, C.S.; Chen, D.; Lu, X.; Wang, F.; Zeng, E.Y. Interaction of Toxic Chemicals with Microplastics: A Critical Review. *Water Res.* **2018**, *139*, 208–219. [[CrossRef](#)] [[PubMed](#)]
106. Ferrer, M.; Chernikova, T.N.; Yakimov, M.M.; Golyshev, P.N.; Timmis, K.N. Chaperonins Govern Growth of *Escherichia Coli* at Low Temperatures. *Nat. Biotechnol.* **2003**, *21*, 1267. [[CrossRef](#)]
107. Saborowski, R.; Korez, Š.; Riesbeck, S.; Weidung, M.; Bickmeyer, U.; Gutow, L. Shrimp and Microplastics: A Case Study with the Atlantic Ditch Shrimp *Palaemon Varians*. *Ecotoxicol. Environ. Saf.* **2022**, *234*, 113394. [[CrossRef](#)] [[PubMed](#)]
108. Scherer, C.; Brennholt, N.; Reifferscheid, G.; Wagner, M. Feeding Type and Development Drive the Ingestion of Microplastics by Freshwater Invertebrates. *Sci. Rep.* **2017**, *7*, 17006. [[CrossRef](#)] [[PubMed](#)]
109. Araújo, C.V.M.; Moreira-Santos, M.; Ribeiro, R. Active and Passive Spatial Avoidance by Aquatic Organisms from Environmental Stressors: A Complementary Perspective and a Critical Review. *Environ. Int.* **2016**, *92–93*, 405–415. [[CrossRef](#)] [[PubMed](#)]
110. Chen, Q.; Gundlach, M.; Yang, S.; Jiang, J.; Velki, M.; Yin, D.; Hollert, H. Quantitative Investigation of the Mechanisms of Microplastics and Nanoplastics toward Zebrafish Larvae Locomotor Activity. *Sci. Total Environ.* **2017**, *584–585*, 1022–1031. [[CrossRef](#)] [[PubMed](#)]
111. Yin, L.; Chen, B.; Xia, B.; Shi, X.; Qu, K. Polystyrene Microplastics Alter the Behavior, Energy Reserve and Nutritional Composition of Marine Jacopever (*Sebastes schlegelii*). *J. Hazard. Mater.* **2018**, *360*, 97–105. [[CrossRef](#)] [[PubMed](#)]

112. Laist, D.W. Overview of the Biological Effects of Lost and Discarded Plastic Debris in the Marine Environment. *Mar. Pollut. Bull.* **1987**, *18*, 319–326. [[CrossRef](#)]
113. Rehse, S.; Kloas, W.; Zarfl, C. Short-Term Exposure with High Concentrations of Pristine Microplastic Particles Leads to Immobilisation of *Daphnia Magna*. *Chemosphere* **2016**, *153*, 91–99. [[CrossRef](#)] [[PubMed](#)]
114. Wright, S.L.; Rowe, D.; Thompson, R.C.; Galloway, T.S. Microplastic Ingestion Decreases Energy Reserves in Marine Worms. *Curr. Biol.* **2013**, *23*, R1031–R1033. [[CrossRef](#)] [[PubMed](#)]
115. Karami, A.; Romano, N.; Galloway, T.; Hamzah, H. Virgin Microplastics Cause Toxicity and Modulate the Impacts of Phenanthrene on Biomarker Responses in African Catfish (*Clarias gariepinus*). *Environ. Res.* **2016**, *151*, 58–70. [[CrossRef](#)] [[PubMed](#)]
116. Von Moos, N.; Burkhardt-Holm, P.; Köhler, A. Uptake and Effects of Microplastics on Cells and Tissue of the Blue Mussel *Mytilus edulis* L. after an Experimental Exposure. *Environ. Sci. Technol.* **2012**, *46*, 11327–11335. [[CrossRef](#)] [[PubMed](#)]
117. Ogonowski, M.; Gerdes, Z.; Gorokhova, E. What We Know and What We Think We Know about Microplastic Effects—A Critical Perspective. *Curr. Opin. Environ. Sci. Health* **2018**, *1*, 41–46. [[CrossRef](#)]
118. Anggraini, R.R.; Risjani, Y.; Yanuhar, U. Plastic Litter as Pollutant in the Aquatic Environment: A Mini-Review. *J. Ilm. Perikan. Dan Kelaut.* **2020**, *12*, 167–180. [[CrossRef](#)]
119. Queiroz, L.G.; Rani-Borges, B.; Prado, C.C.A.; de Moraes, B.R.; Ando, R.A.; de Paiva, T.C.B.; Pompêo, M. Realistic Environmental Exposure to Secondary PET Microplastics Induces Biochemical Responses in Freshwater Amphipod *Hyalella Azteca*. *Chem. Ecol.* **2023**, *39*, 288–301. [[CrossRef](#)]

Disclaimer/Publisher’s Note: The statements, opinions and data contained in all publications are solely those of the individual author(s) and contributor(s) and not of MDPI and/or the editor(s). MDPI and/or the editor(s) disclaim responsibility for any injury to people or property resulting from any ideas, methods, instructions or products referred to in the content.